Ultrafast Time-Evolution of the Nonlinear Susceptibility of Hot Carriers at the Ge(111)−GeO_2 Interface As Probed by SHG

Arthur McClelland, Vasiliy Fomenko, and Eric Borguet*

Department of Chemistry & Surface Science Center, University of Pittsburgh, Pittsburgh, Pennsylvania 15260

Received: July 30, 2003; In Final Form: September 20, 2003

Time-resolved second harmonic generation (SHG) was used to study hot carrier dynamics at the Ge(111)−GeO_2 interface on the femtosecond time scale. A linear dependence of the change in SHG on the pump power was observed for the carrier density range of 3×10^{18} to 2.2×10^{19} cm^{-3}. The ratio of the hot carrier to valence band nonlinear susceptibilities was determined to be 924 ± 40 in the Ge(111)−GeO_2 system, an order of magnitude greater than for Si(111)−SiO_2. The dynamic SHG response is attributed to a change in the nonlinear susceptibility of the excited carriers and the diffusion of excited carriers away from the interface. The time to reach SHG steady-state response (410 ± 70 fs) appears independent of carrier density in the range explored. The time evolution of the hot carrier nonlinear susceptibilities for Ge(111)−GeO_2 at the $\bar{2}11$ azimuth was extracted and shown to follow a double exponential evolution with time constants of 170 ± 50 fs and 3500 ± 1450 fs, similar to the literature values for bulk scattering times of electrons out of the Γ valley (∼100 fs) and into the L valley (∼3.7 ps).

Introduction

Understanding carrier dynamics at semiconductor interfaces is important in many physical and chemical processes of fundamental scientific and technological interest. Hot carriers, i.e., carriers with excess kinetic energy relative to the lattice, can play a significant role in degradation of the insulating gate oxide in MOSFETs.[1,2] In addition, knowledge of carrier relaxation rates is important for the correct modeling of the operation of semiconductor devices.[3] The relaxation rate of hot carriers is a measure of how fast energy can be transferred from the hot carriers to the lattice. Processes involving atomic motion such as ablation, etching, melting, and phase transitions subsequently use this lattice energy.[4] Carrier dynamic information would also be useful in understanding and designing photodriven material processing techniques. The relaxation rate of photoexcited carriers determines the yield in surface photochemical reactions such as photolithography.[5] Recently there has been renewed interest in Ge devices due to the potential for faster devices from the higher carrier mobility of Ge relative to Si.[6,7] However, the hot carrier dynamics at the Ge-dielectric interface are not well-known. The experiments described here were aimed specifically at understanding the behavior of carriers at the Ge−insulator interface on the femtosecond (10^{-15} s) time scale after their creation with ∼0.8 eV of excess energy.

Many different experimental techniques have been used to study carrier dynamics in semiconductors. They include transient reflectivity,[8,9] transient grating,[5] differential optical transmission,[10−12] and transient Raman scattering.[13,14] A limitation of all of these techniques is that they are not specifically sensitive to the interface. To observe the dynamics of carriers that are at the semiconductor−dielectric interface, time-resolved second harmonic generation (SHG), an interface-specific probe, was chosen.[15−18]

* Author to whom correspondence should be addressed. E-mail: borguet@pitt.edu.

Experimental Section

The SHG experiments reported here were performed with a ∼100 fs, 76 MHz Ti:sapphire oscillator (Coherent Mira Seed) operating at 800 nm as described elsewhere.[19] The probe and the pump beam passed, symmetrically off axis, through a 100 mm lens that focused the beams to a 30 ± 4 μm diameter spot. The typically s-polarized pump power was 150 mW, corresponding to an excited carrier density of 1.8×10^{19} cm^{-3}. The p-polarized probe power was 50 mW, corresponding to an excited carrier density 9×10^{18} cm^{-3}. Since the pump struck the sample at an angle of 47° and the probe struck the sample at 43°, the beams formed ellipses on the sample. This has been taken into account in calculating the focused beam area in the carrier density calculations. All experiments were performed at 295 K, in laboratory ambient air.

The pump beam delay was controlled by a stepper motor driven translation stage. The data were collected in 80 fs steps with a collection time of 1 s/point. Typically, 10 scans were averaged to improve the S/N ratio. All scans were performed with the Ge crystal oriented to a major maximum of the SHG rotational anisotropy with p-polarized light.[19,20]

Ge wafers (undoped, Eagle Picher) were degreased by successive 10 min sonication in trichloroethylene (J. T. Baker, reagent grade), acetone (EM Science, reagent grade), then methanol (Fisher Scientific, certified ACS grade). No additional treatment was performed on oxidized samples before experiments. All chemicals were used as received. The oxide was determined to be ∼2.3 nm thick from ellipsometric measurements, using extrapolated optical constants $n = 5.505$ and $k = 0.776$ for Ge[21] and $n = 1.604$ for GeO_2.[22,23]

Results

(a) Determination of the Second-Order Nonlinear Susceptibility of Photogenerated Electron Hole Pairs in Ge(111)−GeO_2. The results of a typical pump−probe SHG experiment from the Ge(111)−GeO_2 interface are illustrated in

10.1021/jp036231k CCC: $27.50
Published on Web 03/02/2004

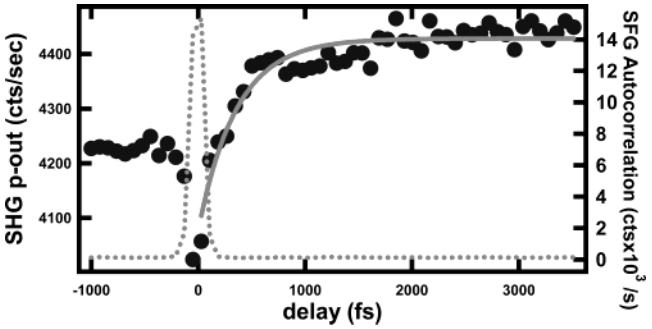

Figure 1. SHG pump−probe Ge(111)−GeO_2 in p_{in}-p_{out} configuration, s-pump 150 mW, p-probe 50 mW. The dotted line is the sum frequency generation (SFG) autocorrelation. Solid line is a single-exponential fit used to determine τ. $\tau = 358 \pm 35$ fs. Bleach 5% ± 0.5%

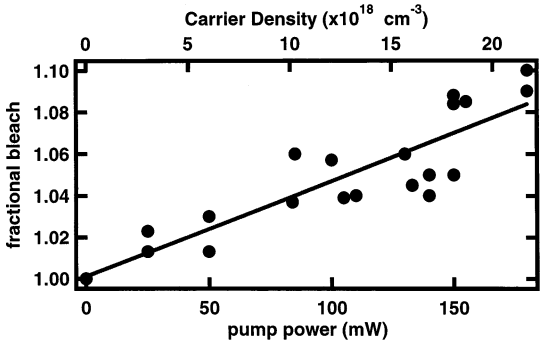

Figure 2. Fractional bleach vs pump power. $\chi^{*(2)}/\chi^{(2)} = 924 \pm 40$ in the Ge(111)−GeO_2 system data was taken with a p-polarized pump and s-polarized probe. Solid line is a fit to eq 3.

Figure 1. Generally, a prompt dip in the SHG signal is observed around $t = 0$, followed by an exponential increase in signal at $t > 0$ to a final steady-state level.

The increase in the SHG signal for $t > 0$ can be understood as an increase in the $\chi^{(2)}$ of the system. The electrons in the valence band can be considered to be bound as in a dielectric. The electrons in the conduction band can be considered to be quasi-free as in a metal. The polarizability of quasi-free electrons is greater than that of bound electrons.[24] At $t > 0$ there are more electrons in the conduction band than at $t < 0$, so the second harmonic signal will be greater at $t > 0$, provided that the nonlinear susceptibilities add in phase.[15]

The pump-induced change in the linear optical properties via the Fresnel coefficients at ω and 2ω can also change the SHG response. This contribution, in the absence of changes in the nonlinear optical properties, was calculated to result in an increase in SHG, but accounts for at most 1/10 of the increase in SHG signal. The change in the nonlinear optical properties must account for the remaining 9/10 of the change in signal.

A linear dependence of the bleach, defined as the change between the initial ($t < 0$) and final ($t > 0$) steady-state signal levels, on pump power was observed for Ge in the carrier density ranges of 3×10^{18} to 2.2×10^{19} cm^{-3} (Figure 2). In the simplest approximation one assumes that the total second-order nonlinear susceptibility of the system, $\chi_s^{(2)}$, depends on the carrier density in the excited state and the unexcited state in the following manner:

$$\chi_s^{(2)} = N\chi^{(2)} + N^*\chi^{*(2)} \tag{1}$$

where N^* and N are the photoexcited e−h pair density and the valence band electron density, respectively, and $\chi^{*(2)}$ and $\chi^{(2)}$ are the nonlinear susceptibilities of the photoexcited carriers and valence band electrons, respectively.[15] At $t < 0$ the only photoexcited carriers, N^*_{probe}, are those excited by the probe pulse.[15] At $t > 0$ photoexcited carriers, N^*_{all}, from both the pump and the probe contribute to the signal. One can take the normalized change in SHG signal as

$$\frac{I(t > 0)}{I(t < 0)} = \frac{|N^*_{all}\chi^{*(2)} + N\chi^{(2)}|^2}{|N^*_{probe}\chi^{*(2)} + N\chi^{(2)}|^2} \tag{2}$$

where $I(t > 0)$ is the SHG steady state at long times, taken to be the last picosecond of the scan. $I(t < 0)$ is the SHG intensity from the surface unperturbed by the probe.

The ratio $I(t > 0)/I(t < 0)$ depends quasi-linearly on input pump power under our experimental conditions (Figure 2). The data (ratio $I(t > 0)/(I(t < 0))$ was fit to

$$\frac{I(t > 0)}{I(t < 0)} = \frac{1 + 2\frac{N^*_{all}}{N}\frac{\chi^{*(2)}}{\chi^{(2)}} + \left(\frac{N^*_{all}}{N}\right)^2\left(\frac{\chi^{*(2)}}{\chi^{(2)}}\right)^2}{1 + 2\frac{N^*_{probe}}{N}\frac{\chi^{*(2)}}{\chi^{(2)}} + \left(\frac{N^*_{probe}}{N}\right)^2\left(\frac{\chi^{*(2)}}{\chi^{(2)}}\right)^2} \tag{3}$$

a simplified expansion of eq 2, using the ratio of $\chi^{*(2)}/\chi^{(2)}$ as the only fit parameter. In eq 3, $N^*_{all} = N^*_{probe} + N^*_{pump}$, $N = 2 \times 10^{23}$ cm^{-3}—the carrier density of the valence band, estimated as (Ge atomic density × 4), $N^*_{probe} = 9 \times 10^{18}$ cm^{-3}—the carrier density photoexcited by the probe. An in-phase relationship of the excited- and ground-state contributions to SHG is assumed. The increase in SHG at $t > 0$ justifies this assumption for the Ge(111)−GeO_2 system.

The curve fit yields 462 ± 20 for the $\chi^{*(2)}/\chi^{(2)}$ ratio in the Ge(111)−GeO_2 system. These numbers were calculated using the initial excited carrier density. However, when $I(t > 0)$ is evaluated at 2.5−3.5 ps, our calculations of the carrier density re-distribution due to diffusion show that half the carriers excited by the pump have diffused into the bulk, out of the region probed by SHG after 2−3 ps. (The carrier diffusion calculations are addressed in section b below.) Taking this into account, by reducing N^*_{all} by a factor of 2, yields a $\chi^{*(2)}/\chi^{(2)}$ ratio of 924 ± 40 in the Ge(111)−GeO_2 system at the SHG steady-state signal level.

The model described by eq 3 starts to deviate significantly from linearity around an excited carrier density of 7×10^{19} cm^{-3}, when the quadratic term is 10% of the linear term and can no longer be ignored.

(**b) Carrier Diffusion.** The effect of hot carrier diffusion into the bulk, due to the excited carrier concentration gradient, was investigated by calculating the spatial distribution of excited carriers as a function of time (Figure 3).[30] The initial pump-induced (150 mW) concentration of carriers is given by eq 4:

$$N_0 = \frac{I_0(1 - R)\alpha}{h\nu} = 1.8 \times 10^{19}\,\mathrm{cm}^{-3} \tag{4}$$

The complex refractive index at 800 nm for Ge is $n = 4.635$ and $k = 0.298$,[21] the reflectivity is $R = 0.3$, the optical penetration depth is 0.2 μm, and the absorption coefficient $\alpha = \frac{4\pi k}{\lambda} = 50501$ cm^{-1}. The surface recombination velocity is taken as $S = 10^2$ cm/s.[25] Values as large as 100 000 cm/s were found not to have a significant effect on the simulations. The ambipolar diffusivity is taken as $D = 65$ cm^2/s.[26] Modeling of hot carrier diffusion indicates that 50% of the carriers excited

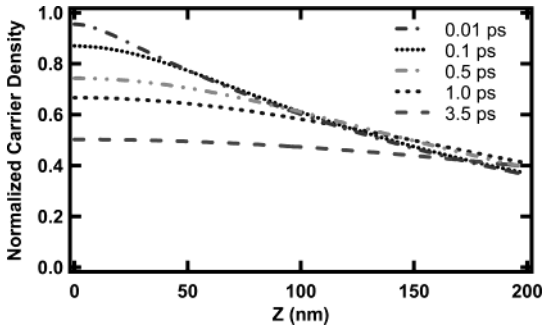

Figure 3. The carrier density as a function of distance from the surface at different times after excitation calculated as described in text. The data are plotted over the penetration depth of the fundamental (800 nm) light in Ge. No bandbending effects are considered since intrinsic Ge was used for experiments.

at $t = 0$ have diffused out of the region probed on the 3.5 ps time scale of the pump−probe experiment, Figure 3.

(c) Interfacial Carrier Dynamics and Evolution of $\chi^{*(2)}$. This rapid depletion of the excited carrier density in the probed region is an interesting and important point. The SHG signal from the pump−probe experiments typically reaches a steady-state level after approximately 1 ps. The change in SHG signal is modulated by the number of excited carriers, N^*, times the $\chi^{*(2)}$ of the system, as can be seen from eq 2. The rapid depletion of excited carriers in the region probed[27] must lead to a decrease in SHG. However, the steady-state level of the SHG signal in the 1−3.5 ps range implies that the $\chi^{*(2)}$ of the system must be evolving in time in such a way as to counteract the loss of excited carriers in the probed region.

Photoinduced variations of the linear optical properties can cause surprisingly large changes in the nonlinear optical response.[28,29] To analyze the change in SHG due to refractive index changes, we adopted a model previously used to describe the time-dependent linear optical properties of semiconductors.[8,30] The linear optical properties depend on the temperature, carrier concentration, and indices of refraction for 800 and 400 nm light. The effect of linear optical properties on SHG through the Fresnel factors was considered and found to account for <1/10 of the change in the signal. We can conclude that 9/10 of the transient SHG signal is due to changes in the nonlinear optical properties.

The laser pulses can heat the sample and change the nonlinear optical response, again through changes in Fresnel factors. Each laser pulse initially heated the sample by 2.6 K.[31] The cumulative heating effects were calculated to rapidly reach steady state with a ~70 K temperature rise.[31] In the experiments reported here, no significant drift of the initial and final signal levels in successive scans was observed, suggesting that the samples had reached steady-state temperature and that changes in SHG are due to reasons other than laser-induced heating.

Our analysis agrees with SHG behavior observed for other hot carrier systems. For example, in a time-resolved SHG probe of electron relaxation processes in Au, following intense 800 nm excitation, Guo et al. revealed an enhancement in $\chi^{(2)}$ at ~300 fs after laser excitation, attributed to thermalization of hot electrons.[28] Guo et al. found that $\chi^{(2)}_{eff}$ was much higher for an equilibrium electron distribution than for the nonequilibrium electron distribution that exists immediately after pump excitation.[28] We observed a similar behavior of $\chi^{(2)}$ in Ge(111)−GeO_2.

The dip in signal near $t = 0$ in the cross-polarized configuration could in fact be a manifestation of this phenomenon. The electrons immediately after $t = 0$ are in a "nonequilibrium" state

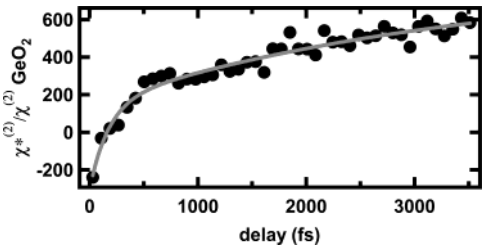

Figure 4. Time evolution of the $\chi^{*(2)}$ (t)/$\chi^{(2)}$ ratio for the Ge(111)−GeO_2 interface extracted from data in Figure 1.

that has a $\chi^{*(2)}$ that is actually out of phase with the $\chi^{(2)}$ of the unexcited electrons. This leads to a lower overall SHG signal at $t = 0$ than at the end of pump-probe scan, when the equilibrium $\chi^{*(2)}$ is in phase with the unexcited valence band electrons.

Guo et al. suggested that the efficiency of the SHG process is proportional to an electron distribution function involving initial, intermediate, and final density of states.[28] We suggest that the $\chi^{*(2)}/\chi^{(2)}$ ratio increases when electrons scatter from the Γ valley to the X valley, due to the larger density of available states in the X valley compared to the Γ valley.[9,32] The diffusion of electrons into the bulk will reduce the state filling in X valley, further increasing the density of available states.

We suggest that the transient response is related to a change in $\chi^{*(2)}$, the nonlinear susceptibility of the hot carriers, which in turn is related to the thermalization of hot electrons.[28] The Auger recombination time, calculated to be 13 ns in Ge at a carrier density of 1.8×10^{19} cm^{-3}, is much too slow to be observed in these experiments.[13] Electron−hole scattering, which occurs on the order of 10^{-13} s, allows the electron and hole systems to reach thermal equilibrium by energy transfer to the crystal lattice.[13] Most of the excess energy is in the electron system, rather than the hole system, due to the lower effective mass of the electron.

The behavior of the $\chi^{*(2)}/\chi^{(2)}$ ratio (see Figure 4), reveals the density of states available to an electron at the surface increases as a function of time. The data in Figure 4 was fit to a double exponential $830-680\exp(-t/3500) - 450\exp(-t/170)$. These time constants are surprisingly close to those reported for the scattering of hot electrons in bulk Ge.[9] The fast time constant can be attributed to the scattering of the electrons from the Γ valley to the X valley with the larger density of states, about 100 fs in bulk Ge.[9,32] The slower time constant is probably a convolution of changes in $\chi^{*(2)}$ due to the cooling of the carriers and the scattering of the electrons to the L valley, reported to be 3.7 ps in the bulk. The similarity of the observed time scales with bulk electron dynamics suggests that the nonlinear optical response is dominated by electrons rather than holes and that the presence of an ultrathin dielectric GeO_2 layer at the interface does not alter the electron dynamics significantly.

Interfacial charge trapping is an important channel for excited carriers and is particularly relevant to semiconductor nanoparticles where the interface can dominate carrier dynamics.[33] In principle, charge trapping at the interface could give rise to the observed steady-state SHG signal. This hypothesis was investigated by taking longer pump−probe scans. The long-term decrease of the SHG response, Figure 5, does not support significant charge trapping at the interface. Rather it suggests that the dynamics are governed by diffusion. To test this hypothesis, the SHG signal was modeled for the situation where the number of excited carriers probed was fixed, due to trapping, at the initial carrier density (dashed line) and at the carrier density remaining at the interface after 3.5 ps (dotted line). The

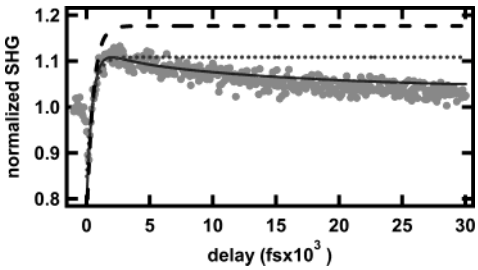

Figure 5. Long time scale SHG dynamics for Ge(111)−GeO_2 and comparison of modeling of SHG response for the scenario where all excited carriers are trapped (dashed line), the charge trapping scenario at 3.5 ps (dotted line), and the carrier diffusion scenario (solid line).

solid line represents the SHG response when the excited carriers were allowed to continue diffusing away from the surface. In all cases $\chi^{*(2)}$ was allowed to evolve (as a double exponential based on the analysis presented above).

The modeling of carrier trapping (Figure 5) is based on the assumption that the second-order nonlinear susceptibility ($\chi^{(2)}$) for trapped carriers is similar to that of free carriers. However, the trap states should be more localized than the delocalized excited state, and the second-order nonlinear susceptibility of trapped electrons might more closely resemble that of the localized ground state. Therefore, it would appear that the SHG response should decrease with trapping, a behavior that would also be consistent with the experimental observation. On the other hand, trapping would result in the buildup of fixed charge at the Ge(111)/GeO_2 interface and a concomitant build up of EFISH. We believe that this would modulate the SHG response even more dramatically than the injection of excited carriers into the conduction band. The second-order nonlinear susceptibility per trapped electron for Si(111)/SiO_2 is orders of magnitude greater than the response per electron of photoexcited carriers. EFISH signals associated with 10^{12} e/cm^2 trapped in the SiO_2 result in an order of magnitude increase in SHG.[34−36] In the experiments reported here, 10^{19} e/cm^3 photoexcited carriers were injected into a probe depth of 10^{-6} cm, i.e., 10^{13} e/cm^2. The preceding discussion, coupled with the success in modeling the observed behavior with bulk diffusion constants, suggests that electron diffusion into the bulk, rather than electron trapping at the interface, is the dominant cause of the observed long time scale behavior of the SHG dynamics, Figure 5.

Conclusions

The dynamics of hot carriers, with 0.8 eV excess energy, at the Ge(111)−GeO_2 interface were investigated by ultrafast pump probe SHG. The susceptibility of the initial nonequilibrium distribution of excited carriers, $\chi^{*(2)}$, is initially out of phase with the susceptibility of the unexcited Ge(111)−GeO_2 system. As an equilibrium excited carrier distribution is established the $\chi^{*(2)}$ changes to be in phase with the $\chi^{(2)}$ of the unexcited system, leading to the observed increase in SHG signal. The excited carrier gradient drives the diffusion of the hot carriers away from the interface. Concomitantly, the $\chi^{*(2)}/\chi^{(2)}$ was found to increase so that within a few picoseconds the $\chi^{*(2)}/\chi^{(2)}$ ratio reached a value of 924 ± 40, an order of magnitude greater than for Si(111)−SiO_2.[15] The biexponential dynamics of the $\chi^{*(2)}/\chi^{(2)}$ ratio involve a significant (40%) ultrafast evolution on a time scale of about 170 fsec, followed by a slower (3.5 ps) component. The time scales suggest that the SHG at 800 nm probes electron rather than hole dynamics. The data does not support charge trapping at the interface. Instead diffusion appears to dominate the observed temporal evolution of the SHG response at longer times (>3 ps).

Acknowledgment. The authors acknowledge the generous support of the DOE, Office of Basic Energy Sciences.

References and Notes

(1) Hess, K.; Register, L. F.; McMahon, W.; Tuttle, B.; Aktas, O.; Ravaioli, U.; Lyding, J. W.; Kizilyalli, I. C. Theory of channel hot-carrier degradation in MOSFETs. *Physica B* **1999**, *272* (1−4), 527−531.

(2) Cheng, K.; Lee, J.; Hess, K.; Lyding, J.; Kim, Y.; Kim, Y.; Suh, K. Improved Hot-Carrier Reliability of SOI Transistors by Deuterium Passivation of Defects at Oxide/Silicon Interfaces. *IEEE-Trans. Electron Devices* **2002** *49* (3), 529−531.

(3) Fischetti, M. V.; Laux, S. E.; Crabbe, E. Understanding hot-electron transport in silicon devices: Is there a shortcut? *J. Appl. Phys.* **1995**, *78* (2), 1058−1087.

(4) Sjodin, T.; Li, C. M.; Petek, H.; Dai, H. L. Ultrafast transient grating scattering studies of carrier dynamics at a silicon surface. *Chem. Phys.* **2000**, *251*, 205−213.

(5) Sjodin, T.; Petek, H.; Dai, H. L. Ultrafast carrier dynamics in silicon: A two-color transient reflection grating study on a Si(111)surface. *Phys. Rev. Lett.* **1998**, *81* (25), 5664−5667.

(6) Chui, C.; Kim, H.; Chi, D.; Triplett, B.; McIntyre, P.; Saraswat, K. A sub-400 degree C Germanium MOSFET Technology with High -k dielectric and Metal Gate. In *International Electron Devices Meeting (IEDM) '02*. 2002: IEEE.

(7) Shang, H.; Okorn-Schmidt, H.; Chan, K.; Copel, M.; Ott, J.; Kozlowski, P.; Steen, S.; Cordes, S.; Wong, H.; Jones, E.; Haensch, W. High Mobility p-channel Germanium MOSFETs with a thin Ge Oxynitride Gate Dielectric. In *International Electron Devices Meeting (IEDM)*. 2002: IEEE.

(8) Sabbah, A. J.; Riffe, D. M. Measurements of silicon surface recombination velocity using ultrafast pump−probe reflectivity in the near-infrared. *J. Appl. Phys.* **2000**, *88* (11), 6954−6956.

(9) Zollner, S.; Myers, K. D.; Jensen, K. G.; Dolan, J. M.; Bailey, D. W.; Stanton, C. J. Femtosecond Interband Hole Scattering in Ge Studied by Pump−Probe Reflectivity. *Solid State Commun.* **1997**, *104* (1), 51−55.

(10) Bailey, D. W.; Stanton, C. J. Calculations of femtosecond differential optical transmission in germanium. *J. Appl. Phys.* **1995**, *77* (5), 2107−2115.

(11) Zhou, X. Q.; van Driel, H. M.; Mak, G. Femtosecond kinetics of photoexcited carriers in germanium. *Phys. Rev. B* **1994**, *50* (8), 5226−5230.

(12) Mak, G.; van Driel, H. M. Femtosecond transmission spectroscopy at the direct band edge of germanium. *Phys. Rev. B* **1994**, *49* (23), 16817−16820.

(13) Othonos, A. Probing ultrafast carrier and phonon dynamics in semiconductors. *J. Appl. Phys.* **1998**, *83* (4), 1789−1830.

(14) Tanaka, K.; Ohtake, H.; Nansei, H.; Suemoto T. Subpicosecond Hot-Hole Relaxation in Germanium Studied by Time- Resolved Inter-Valence-Band Raman-Scattering. *Phys. Rev. B* **1995**, *52* (15), 10709−10712.

(15) Bodlaki, D.; Borguet, E. Dynamics and Second-Order Nonlinear Optical Susceptibility of Photoexcited Carriers at Si(111) Interfaces. *Appl. Phys. Lett.* **2003**, *83*, 2357−2359.

(16) Downer, M. C.; Mendoza, B. S.; Gavrilenko, V. I. Optical second harmonic spectroscopy of semiconductor surfaces: advances in microscopic understanding. *Surf. Interface Anal.* **2001**, *31* (10), 966−986.

(17) Lupke, G. Characterization of semiconductor interfaces by second-harmonic generation. *Surf. Sci. Rep.* **1999**, *35* (75), 75−161.

(18) Sipe, J. E.; Moss, D. J.; van Driel, H. M. Phenomenological theory of optical second- and third-harmonic generation from cubic centrosymmetric crystals. *Phys. Rev. B* **1987**, *35* (3), 1129.

(19) Fomenko, V.; Bodlaki, D.; Faler, C.; Borguet, E. Second Harmonic Generation from chemically modified Ge (111) Interfaces. *J. Chem. Phys.* **2002**, *116* (15), 6745−6754.

(20) Bodlaki, D.; Yamamoto, H.; Waldeck, D. H.; Borguet, E. Ambient Stability of Chemically Passivated Germanium Interfaces. *Surf. Sci.* **2003**, *543*, 63−74.

(21) *Handbook of Chemistry and Physics*, 78th ed.; Lide, D., Ed.; CRC Press: Boca Raton, 1998.

(22) Vega, F.; de Sande, J. C. G.; Afonso, C. N.; Ortega, C.; Siejka, J. Optical properties of GeO_x films obtained by laser deposition and dc sputtering in a reactive atmosphere. *Appl. Opt.* **1994**, *33* (7), 1203.

(23) Caperaa, C.; Baud, G.; Besse, J. P.; Bondot, P.; Fessler, P.; Jacquet, M. Preparation and characterization of germanium oxide thin films. *Mater. Res. Bull.* **1989**, *24*, 1361.

(24) Shen, Y. R. *Principles of Nonlinear Optics*; Wiley: New York, 1984.

(25) Ponpon, J. P. Evolution with time of the surface properties of high-purity germanium. *Nucl. Instrum. Methods Phys. Res., Sect. A* **2001**, *457*, 262−265.

(26) Chigarev, N. V.; Yu, D.; Parashchuk; Yu.; Pan, S.; Gusev, V. E. Laser Hyperacoustic Spectroscopy of Single-Crystal Germanium. *J. Exp. Theor. Phys.* **2002**, *94* (3), 627−636.

(27) Othonos, A.; van Driel, H. M.; Young, J.; Kelly, P. Correlation of hot-phonon and hot carrier kinetics in Ge on a picosecond time scale. *Phys. Rev. B* **1991**, *43* (8), 6682−6690.

(28) Guo, C.; Rodriguez, G.; Taylor, A. J. Ultrafast dynamics of electron thermalization in gold. *Phys. Rev. Lett.* **2001**, *86* (8), 1638.

(29) Sokolowski-Tinten, K.; Bialkowski, J.; von der Linde, D. Ultrafast laser-induced order−disorder transitions in semiconductors. *Phys. Rev. B* **1995**, *51* (20), 14186.

(30) Tanaka, T.; Harata, A.; Sawada, T. Subpicosecond surface-restricted carrier and thermal dynamics by transient reflectivity measurements. *J. Appl. Phys.* **1997**, *82* (8), 4033−4038.

(31) Dadap, J. I.; Hu, X. F.; Russell, N. M.; Ekerdt, J. G.; Lowell, J. K.; Downer, M. C. Analysis of second-harmonic generation by unamplified, high- repetition-rate, ultrashort laser pulses at Si(001) interfaces. *IEEE J. Selected Top. Quantum Electron.* **1995**, *1* (4), 1145−1155.

(32) Zollner, S.; Myers, K. D.; Dolan, J. M.; Bailiey, D. W.; Stanton, C. J. Theory of femtosecond ellipsometry in Ge at 1.5 eV. *Thin Solid Films* **1998**, *313*−*314*, 568−573.

(33) Zhang, J. Interfacial Charge Carrier Dynamics of Colloidal Semiconductor Nanoparticles. *J. Phys. Chem. B* **2000**, *104*, 7239−7253.

(34) Aktsipetrov, O. A.; Fedyanin, A. A.; Melnikov, A. V.; Dadap, J. I.; Hu, X. F.; Anderson, M. H.; Downer, M. C.; Lowell, J. K. Dc electric field induced second-harmonic generation spectroscopy of the Si(001)−SiO_2 interface: Separation of the bulk and surface nonlinear contributions. *Thin Solid Films* **1997**, *294* (1−2), 231−234.

(35) Mihaychuk, J. G.; Bloch, J.; Liu, Y.; van Driel, H. M. Time-Dependent Second-Harmonic Generation From the Si−SiO_2 Interface Induced By Charge-Transfer. *Opt. Lett.* **1995**, *20* (20), 2063−2065.

(36) Fomenko, V.; Hurth, C.; Ye, T.; Borguet, E. Second harmonic generation investigations of charge transfer at chemically modified semiconductor interfaces. *J. Appl. Phys.* **2002**, *91* (7), 4394−4398.